ARCHIVES OF ELECTRICAL ENGINEERING VOL. 73(4), pp. 849–867 (2024)

DOI 10.24425/aee.2024.152099

Modeling of air transformers integrating ferrite plates for improved performance

KRZYSZTOF GÓRECKI ✉, KALINA DETKA

Faculty of Electrical Engineering, Gdynia Maritime University
81-87 Morska St., 81-225 Gdynia, Poland
e-mail: {✉ k.gorecki/k.detka}@we.umg.edu.pl

(Received: 27.03.2024, revised: 12.11.2024)

Abstract: This article proposes a model of an air transformer taking into account the influence of the use of ferrite plates on properties of such a transformer. This model has the form of a subcircuit dedicated for the SPICE software. It takes into account the influence of such parameters as the number of turns of both windings, the distance between them, the parasitic capacitances of the windings and the sizes of the ferrite plates used on the voltage ratio and frequency characteristics of the air transformer. The form of the developed model is described and some results illustrating the practical usefulness of this model are shown. The obtained results of calculations performed with the use of the proposed model are compared with the corresponding measurement results.

Key words: air-core transformer, ferrite plates, modeling, SPICE, wireless power transfer

1. Introduction

Transformers can be found in almost every power electronic system [1]. Typically, they contain a ferromagnetic core, on which the windings are wound [2, 3]. Most often, they are used to ensure galvanic separation between electrical circuits and when it is necessary to adjust the power supply parameters to the receiver parameters [2]. Transformers are also used in systems for wireless power transfer (WPT) [4–6], but in this case they typically do not contain a ferromagnetic core, on which the windings are wound [7, 8].

Transformers used in WPT systems contain transmitting and receiving coils. The lack of a core in such transformers means that they are characterized by lower energy efficiency compared with a traditional transformer with a core as a result of weaker magnetic coupling between the mentioned coils.

Wireless power supply systems are becoming more and more popular thanks to the ability to transfer more and more energy between transformer coils. According to the literature [9–11], the IPT (Inductive Power Transfer) technology is the most efficient in power transfer between transformer coils. Compared with other technologies, the efficiency of power transfer using the mentioned technology reaches up to 90% [9–11]. Additionally, in the papers [12–18] it was shown that the WPT system properties in the IPT technology, including the efficiency of power transfer, are influenced by many factors such as: the mutual position of the transmitting and receiving coils, the shape of these coils and the type of the winding used.

In paper [16] it was shown that changing the vertical distance between the transformer coils from 15 mm to 160 mm causes a threefold reduction in the coupling coefficient value. In turn, a change in the horizontal distance between the coils by approximately 200 mm causes a decrease in the considered coefficient value by 60%.

WPT systems designed in accordance with the Qi standard are dedicated to charge batteries with a power of up to 15 W at a distance of up to 4–5 cm [19, 20]. The use of ferrite plates allows increasing the coupling coefficient between the coils of the air transformer. However, typically the ferrite plates used in the Qi standard are small in size. Nevertheless, the offer of the leading producers of ferrite plates, e.g. KEMET [21, 22], includes ferrite plates of much larger sizes. They are designed to operate at higher powers than typical Qi devices and are used, e.g. in the automotive and manufacturing industries.

The offer of ferromagnetic core producers includes ferrite cores dedicated to WPT systems in the form of rectangular, square or round ferrite plates of various sizes [23, 24]. The purpose of the use of these plates is to increase the efficiency of power transfer by increasing a magnetic coupling coefficient between the windings.

According to the literature, the use of ferromagnetic cores in the construction of transformers used in WPT systems affects their properties. For example, in [25] the influence of voltage frequency and the type of the material used to build the ferromagnetic core on the efficiency of WPT was analyzed. The tests were done for systems containing 4 different ferromagnetic cores, i.e. Ni-Zn, Sendust, Irondust, ferrite. In the cited paper it was noted that the highest efficiency was achieved by using the ferrite material.

In turn, in [26] a new construction of the ferrite core was proposed in the form of radial geometry (in the form of ferrite pillars spaced from each other forming a ring). The influence of the proposed geometry on properties of the air transformer and the WPT system was analyzed.

The cited papers indicate that the issue related to the use and selection of an appropriate ferrite core is important from the point of view of ensuring the most effective WPT. It is also desirable to formulate models that take into account various circuit parameters, including ferrite plates, and the influence of their parameters on properties of WPT systems, especially high-power ones.

There are many models of air transformers available in the literature, e.g. [27–30], but they are usually T-type models or their modifications and are characterized by certain limitations. It is important to notice that the T model is not a standalone model, but rather a form of representation used for analyzing electrical networks. In most WPT applications, tuned circuits with capacitive matching networks are utilized. These capacitors in the matching network are physical and integral to the circuit [31].

For example, in [32] the properties of a resonant WPT system with an air transformer were analyzed. In order to perform the above-mentioned analysis, a transformer was designed with windings made of a Litz wire. Additionally, to minimize the leakage flux in the transformer,

aluminum plates were used on the windings' external surfaces. The model of the transformer itself was formulated in the Ansys Maxwell program. The obtained simulation results were verified by analytical calculations. Using the analysis results, it was found that the WPT transformer transmits power with an efficiency of approximately 95%. This model can be effectively used in WPT applications. However, the cited article only compared the results of computer calculations with the results of analytical calculations, and no experimental tests were carried out to confirm the validity of the model. The problem of the transformer model reduction using the time and frequency domain sensitivity techniques is described in the paper [33].

In turn, in [34] the efficiency of power transfer of an air transformer operating in the IPT technology was analyzed. The classic T model was used to analyze the properties of the considered transformer. Additionally, an analysis of the properties of the considered element was performed using a modification of the T-type transformer model. The modified model included 4 compensating capacitors (2 on the primary side and 2 on the secondary side). The conducted research shows that the highest power transfer efficiency was achieved using the modified T model. However, it was indicated that the equations fitting the transformer's output parameters, such as the output power in this circuit configuration for both the coils, are very complex. However, the research did not take into account the influence of the frequency of the excitation voltage, the distance between the transformer coils and the use of ferrite plates on the properties of the considered component.

The method of modeling an air transformer used in medium voltage DC-DC converter systems is described in [35]. The analyses were carried out for two types of transformers, i.e. with concentric cylindrical coils and flat spiral coils made of solids. Both transformers also included a shielding layer to limit the leakage flux. The analyses were performed using the T model and the finite element method, taking into account eddy currents, skin effect, proximity effect and the impact of harmonics on thermal properties of the considered transformers. The results of the tests were compared with the measurement results and it was shown that both the transformer designs are characterized by similar properties.

In turn, in [36] a method of modeling an efficient wireless power supply system used in implantology was presented. To analyze the properties of the air transformer included in the considered system, a model was used, the circuit representation of which consists of 2 resonators constituting a combination of a series capacitor, resistor and inductor. The first one corresponds to the transmitting coil and the other to the receiving coil. For such a model, a transfer function combining voltage and magnetic field flux was defined. In [37] a method of modeling an air transformer and a WPT system containing such a transformer was presented. However, the research did not take into account the influence of ferrite plates on the properties of this transformer.

In [38], a compact model of a transformer dedicated to the SPICE software was proposed. This model takes into account the influence of many factors such as frequency, load resistance and temperature on properties of the considered component. However, this model was not elaborated and considered for a transformer without a core. The research presented in this paper concerns planar transformers and transformers containing ferromagnetic toroidal cores made of different materials.

In the paper [39] the low- and mid-frequency model of the transformer with resistive load is analysed. Different values of coupling coefficients are considered. The considered model is based on the classical structure and it contains only inductors and resistors, whereas parasitic

capacitances of the windings are neglected. It is shown that in the low- and mid-frequency range, the turns ratio between the windings is a strong function of the coupling coefficient. The theoretical considerations are verified experimentally for a transformer with ferromagnetic core.

In the paper [40] a problem of frequency optimization for a WPT system based on AC resistance evaluation in Litz-wire coil is considered. In the described investigations FEM is used. Analytical formulas describing AC resistance of the winding resistance was formulated.

Paper [41] presents an approximate model for multi-strand wire winding, including Litz-wire winding. The proposed model takes into account the existence of the skin effect and the proximity effect within the Litz-wire bundle between the strands and between the bundles. An influence of frequency on the module and phase of the winding impedance are shown and discussed.

Paper [42] presents a design procedure of high-frequency loosely inductive coupled wireless power transfer (LIC-WPT) system based on class- E^2 dc-dc converter, taking into account the power loss reduction of inverter, coupling part, and rectifier simultaneously. The design procedure proposed in the cited paper makes it possible to reduce power loss in the used air-transformer coupling transmitter and receiver part of the WPT system.

Paper [43] proposes geometrical method to obtain an analytical formula describing the self-capacitance of the winding of a single-layer coupled toroidal inductors. This formula takes into account dimensions of the wire, number of turns and the distance between turns. The correctness of the proposed method was verified for a coupled inductor with toroidal ferrite core.

Paper [44] contains an analysis of ac-to-dc winding resistance ratio of Litz-wire. The model proposed in the cited paper takes into account proximity effect within the bundle and between bundle layers as well as the skin effect. It was shown that these effects are important at a frequency higher than 1 MHz.

Performing simple experimental tests allows you to improve the model and extrapolate the results to an extent that is impossible to perform in the laboratory conditions. This may allow us to propose new solutions and analyze physical phenomena that could not be predicted earlier. So far, the literature lacks models of air transformers that are valid both for those components containing ferrite plates and those operating without them. Such models are needed for the effective analysis and design of systems for wireless power transfer.

The aim of this article is to develop a new model of an air transformer containing rectangular ferrite plates and to experimentally verify it for an air transformer operating with and without ferrite plates. Using this model, the influence of the use of ferrite plates on properties of the air transformer was examined. The performed investigations contain both small-signal properties in a wide range of frequency and large-signal properties for different load resistance and frequency values, as well as different distances between the coils of the transformer. In the experimental part of the investigations as the case study one construction of the transformer coils are considered and only sinusoidal waveform of the transformer input voltage are considered. The tested transformer does not operate in any WPT system.

Section 2 describes the proposed model of an air transformer. The tested transformer and measurement set-up are presented in Section 3. Section 4 contains the obtained calculation and measurement results.

2. Model form

The elaborated model of an air-transformer has the form of a dedicated for the SPICE software. This model is based on the transformer models described in the literature, e.g. [39] and it additionally takes into account such physical phenomena as:

a) parasitic windings' capacitances,
b) mutual capacitance between windings,
c) a distance between coils,
d) properties of the ferrite material used to construct the boards,
e) numbers and thickness of these boards.

The proposed model belongs to the group of compact models. For such models all the properties of the modeled device are described with the electrical network making it possible to compute values or waveforms of current and voltages of each winding taking into account all the mentioned above physical phenomena. It also considers both magnetic and electrical couplings between the windings.

The presented model is dedicated for the analyses of WPT systems operating at a frequency below 1 MHz. Therefore, its form should be as simple as possible. At formulation of this model following assumptions were made:

a) the skin effect is omitted,
b) the proximity effect is omitted,
c) dimensions of coils are much smaller then wavelength of magnetic force,
d) only electrical quantities of the transformer are computed.

The network representation the proposed model is given in Fig. 1.

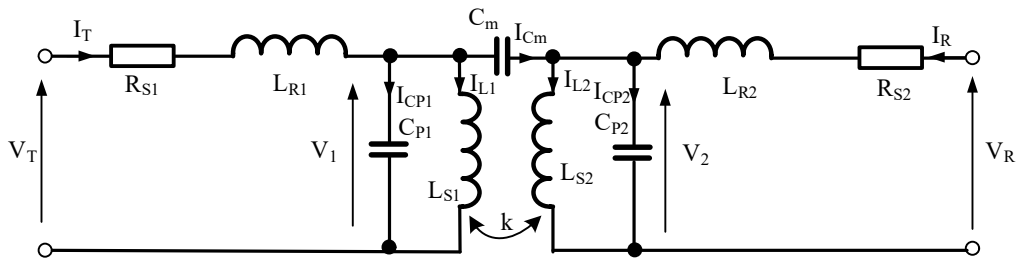

Fig. 1. Network representation of the elaborated model of an air-transformer

The presented model contains two coupled coils L_{S1} and L_{S2} representing the inductance of the transmitting and receiving coils, respectively. These coils are magnetically coupled with each other, and this coupling is characterized by the coupling coefficient k, and capacitively – through the capacitor C_m. Capacitors C_{P1} and C_{P2} represent the parasitic capacitances of each winding. The resistance of the windings is represented by resistors R_{S1} and R_{S2}, respectively. Inductors L_{R1} and L_{R2} describe the leakage inductance of individual windings.

This model takes into account following phenomena: the magnetic coupling between the windings, the parasitic inductances and resistances of the windings. The values of these parameters depend on the distance between the windings and the used ferrite plates. The value of parameter k characterizing the magnetic coupling between both the windings also depends on the distance

d between these windings. An influence of the magnetic force on parameter k is neglected. Therefore, this model is dedicated only for the operating points lying on the linear part of the magnetization characteristic of the used ferrite plate. Practically, the flux density should be lower than one half of saturation flux density. This means that the values of the components occurring in Fig. 1 are constant and they do not depend on voltages and currents of the transformer windings. The equations describing the proposed model contain two groups. The first of them (given by Eqs. (1)–(9) contains network equations describes the network visible in Fig. 1. The other group of equations describe an influence of selected factors on coils inductance, capacitors capacitance and coupling coefficient. These equations are given by Formulas (10)–(13).

The network equations have the form as follows:

$$V_T = I_T \cdot R_{S1} + L_{R1} \cdot \frac{\mathrm{d}I_T}{\mathrm{d}t} + V_1, \tag{1}$$

$$V_1 = L_{S1} \cdot \frac{\mathrm{d}I_{L1}}{\mathrm{d}t}, \tag{2}$$

$$I_{CP1} = C_{P1} \cdot \frac{\mathrm{d}V_1}{\mathrm{d}t}, \tag{3}$$

$$I_{Cm} = C_m \cdot \frac{\mathrm{d}\,(V_1 - V_2)}{\mathrm{d}t}, \tag{4}$$

$$I_T = I_{CP1} + I_{Cm} + I_{L1}, \tag{5}$$

$$V_R = I_R \cdot R_{S2} + L_{R2} \cdot \frac{\mathrm{d}I_R}{\mathrm{d}t} + V_2, \tag{6}$$

$$V_2 = L_{S2} \cdot \frac{\mathrm{d}I_{L2}}{\mathrm{d}t}, \tag{7}$$

$$I_{CP2} = C_{P2} \cdot \frac{\mathrm{d}V_2}{\mathrm{d}t}, \tag{8}$$

$$I_R = I_{CP2} - I_{Cm} + I_{L2}. \tag{9}$$

All the symbols used in Eqs. (1)–(9) are marked in Fig. 1.

In the further part of this section some information about the components of the presented model will give. Eqs. (10)–(13) are formulated on the basis of the performed measurements and selection of mathematical functions describing the obtained experimental dependence.

The values of the series resistance of the windings do not depend on the distance between the windings or on the presence of ferrite plates. In turn, the inductances of L_{S1} and L_{S2} windings depend on the presence of ferrite plates, which increase the value of these inductances by a set value the dimensions of the coil and the numbers of turns [45]. These inductances are described by the following formula:

$$L_{Si} = L_{Si0} + \Delta L_{Si} = a \cdot \mu_0 \cdot \mu_r \cdot D \cdot z^2, \tag{10}$$

where: L_{Si0} is the inductance of L_{Si} coil without a ferrite plate, ΔL_{Si} is an increase in this inductance caused by the use of such a plate, μ_0 is the magnetic permeability of free air, μ_r is the relative permeability of the used plate, D is the average diameter of the turn, z is the number of turns, whereas a is the model parameter. If the coil operates without any ferrite plate μ_r is equal to 1. For the coil with ferrite plate μ_r is higher than 1.

The parasitic capacitances of the windings change when using ferrite plates according to the formula

$$C_{Pi} = C_{Pi0} + \Delta C_{Pi} = b \cdot z \cdot D_w \cdot d_w \cdot \varepsilon, \tag{11}$$

where: C_{Pi0} means the parasitic capacitance of L_{Si} coil without a ferrite plate, ΔC_{Pi} is an increase in this capacity caused by the use of such a plate and b is the model parameter. Both the components of the right side of Eq. (11) are proportional to the number of turns, diameter of the used wire D_w and the distance d_w between adjacent turns. When the ferrite plate is used dielectric permeability ε increases, therefore ΔC_{Pi} has positive value.

Leakage inductances L_{Ri} decrease by the value ΔL_{Ri} when using ferrite plates. Coupling capacitance C_m changes when ferrite plates are used and also depends on the distance d between the windings of both the coils according to the formula

$$C_m = C_{m0} - \Delta C_m - \frac{d}{d_0} \cdot C_{m0}, \tag{12}$$

where: C_{m0} is the coupling capacitance with the distance between windings $d = 0$ and the absence of a ferrite plate, ΔC_m is an increase in this capacitance caused by the use of such a plate, and d_0 is a model parameter. The values of capacitances C_{m0} and ΔC_m are proportional to the area of the coils.

The coupling coefficient k is described by the following empirical formula:

$$k = k_0 + \Delta k - k_1 \cdot \left(1 - \frac{\Delta k_1}{2} \cdot \frac{R_{L0}}{R_L}\right) \cdot \left(1 - \exp\left(\frac{d}{k_2 \cdot (1 + \Delta k_1) \cdot (1 + \alpha_k \cdot (1 + \Delta k_1) \cdot (f - f_0))}\right)\right), \tag{13}$$

where: k_0 is the coupling coefficient of coils in direct contact and not mounted on a ferrite plate, Δk is an increase in the coupling coefficient caused by the use of ferrite plates, f is the frequency, R_L is the load resistance, whereas k_1, k_2, α_k, R_{L0} and f_0 are the model parameters. Formula (13) is inspired by the dependence proposed in [46].

The model described in this section was implemented in the SPICE software as a subcircuit. This model contains inductors, capacitors and resistors connected according to the diagram shown in Fig. 1. The values of these components depend on the numbers of turns of each coil, the distance between them, the dimensions of the coils and the diameter of the used wire. Of course, the values coefficients describing such relationships are different for the transformer operating with a ferrite plate and without such a plate. The parameters of the components occurring in Fig. 1 are given by Eqs. (10)–(13). An influence of the non-linearity of the magnetization curve of the used ferrite plate on the characteristics of the modeled device is neglected. Of course, such simplification limits the range of the usefulness of the presented model. It is dedicated to use for transformer operating without any ferrite plates and for such transformer operating at constant value of magnetic permeability.

The estimation of the model parameters values is indispensable for the practical use of the model. The inductance of each winding can be measured using an RLC bridge for a low value of frequency (about some kilohertz) separately for a winding without any ferrite plate and with this plate. Next, the dependence of the impedance module of each winding on frequency should be measured in order to find the resonance frequency. Using the value of this frequency the parasitic capacitance of each winding can be calculated.

In order to calculate the values of parameters describing the coupling coefficient k, the dependence of the module of the transformer input impedance on frequency should be measured. Such a dependence should be obtained for the transformer operating without any ferrite plate and they with these plates. Particular dependences should be measured for different values of load resistance and different values of the distance between the windings.

The properties of selected models of an air transformer are compared in Table 1.

Table 1. Comparison of properties of selected models

Reference	**Form of the model**	**Output data**	**Experimental verification**	**Ferrite plates included**	**Described measure-ment method**
[47]	FEM	Self-inductance, voltage waveform, output power, magnetic force distribution, current density distribution	yes	no	yes
[12]	FEM	Voltage waveform	yes	no	no
[48]	FEM	Distribution of magnetic flux density, temperature distribution	Temperature only	no	no
[37]	Compact	Transmitter and receiver current and voltage waveform, temperature	yes	no	yes
[49]	Compact	Power transfer efficiency, transmitter and receiver voltage waveforms	yes	no	no
This article	Compact	Transmitter and receiver voltage and current waveforms, module and phase of input impedance	yes	yes	yes

As it is visible, the models described in [12,47,48] are dedicated for the FEM, whereas models described in [37, 49] and in this article belong to the group of compact models. The models dedicated for the FEM make it possible to obtain both the waveforms of voltages and current as well as voltage, temperature and magnetic force distributions. The compact models make it possible to obtain only the waveforms of current and voltages or temperature. Only the model proposed in this article takes into account an influence of ferrite plates.

3. Tested transformer and experimental set-up

In order to verify the model described in the previous section an air transformer was constructed and tested. This transformer contains two spiral windings made of a Litz wire of the diameter equal to 1 mm. Each winding contains 28 turns. These windings have the diameter equal to 75 mm. They are mounted on the ferrite plates in the manner shown in Fig. 2.

The FPL 100/100/4-BH1T ferrite plates used have the dimensions of 100 mm × 100 mm × 4 mm and are made of the BHIT material [50]. The most important parameters of this material have the following values: Initial Permeability μ_i in temperature 23°C is 3000 ± 25%, Core Loss per unit of volume P_{cv} at frequency f = 100 kHz and amplitude of flux density B_m = 200 mT and temperature 23°C is equal to 345 kW/m^3, Curie Temperature Tc = 220°C, Effective Saturation Magnetic Flux Density B_{ms} at H = 1200 A/m and temperature 23°C is equal to 520 mT, Coercive Force = 8.5 A/m.

Fig. 2. Mounting manner of the windings of the tested air transformer on the ferrite plates

The correctness of the obtained results of computations was verified by comparing them with the results of measurements. These measurements were performed using the set-up shown in Fig. 3.

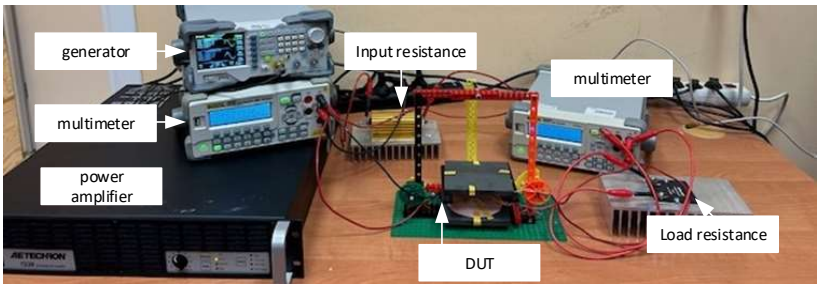

Fig. 3. View of the measurement set-up

In this measurement set-up the windings of the tested transformer (DUT) are arranged horizontally, parallel to each other and supported on a special structure made using 3D printing. This design enables step adjustment of the distance between the windings. The transmitting winding is powered by a sinusoidal signal generated by the power amplifier AETECHRON 7228 and a resistor of resistance 2.2 Ω. The load winding of the receiver is loaded with a power resistor with adjustable resistance. The RMS values of the input and output voltage are measured using RIGOL DM3068 multimeters. In the case of frequency response measurements, the classic RLC bridge from GwInstek was used.

4. Investigation results

In order to verify the correctness of the elaborated model some computations and measurements were performed. The calculation and measurement results are shown in Figs. 4–11. In these figures, the points denote the results of measurements, whereas the lines – the results of calculations obtained with the use of the proposed model. The investigations were carried out for a transformer without and with ferrite plates. In Figs. 4–5 the blue color is used to mark the results obtained for the winding without any ferrite plates, whereas other the colors are used to present the results obtained for windings with 1 ferrite plate (red), 2 ferrite plates (green) and 3 ferrite plates (yellow).

In the performed computations the following values of the model parameters were used: $L_{S10} = 35.4$ µH, $L_{S20} = 33.2$ µH, $\Delta L_{S1} = 179.1$ µH, $\Delta L_{S2} = 161.1$ µH, $L_{R1} = 5$ µH, $L_{R2} = 1.4$ µH, $C_{P10} = 2$ pF, $C_{P20} = 2$ pF, $\Delta C_{P1} = 8$ pF, $\Delta C_{P2} = 8$ pF, $C_{m0} = 1$ nF, $\Delta C_{m0} = 0.5$ nF, $d_0 = 111.1$ mm, $k_0 = 0.88$, $\Delta k = 0.1$, $k_1 = 0.77$, $\Delta k_1 = 0.5$, $R_{L0} = 47$ Ω, $k_2 = 16$, $\alpha_k = 1.5$ µs, $f_0 = 100$ kHz, $R_{S1} = 0.2$ Ω, $R_{S2} = 0.25$ Ω. These values of the mentioned parameters are obtained using the procedure described in Section 2. Next, these values were adjusted to obtain the best possible agreement between the calculation and measurement results.

Figure 4 shows the dependence of the module (Fig. 4(a)) and phase (Fig. 4(b)) of the transmitting winding impedance on frequency. The investigations were carried out for a winding without ferrite plates and with a different number of such plates (from 1 to 3).

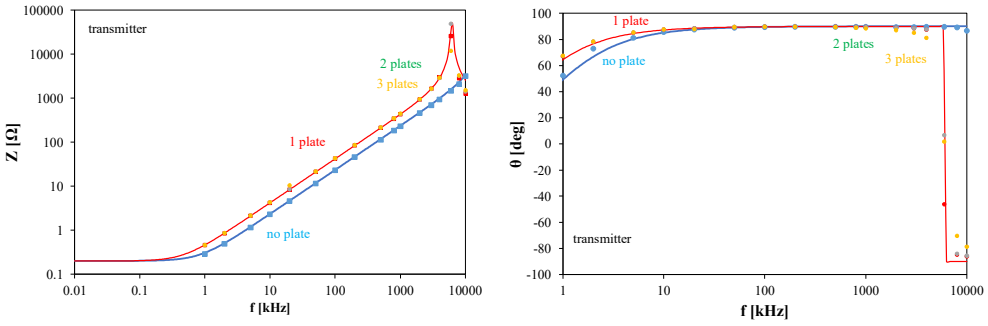

(a) (b)

Fig. 4. Measured and computed dependence of the module (a) and phase (b) of the of the transmitter winding impedance on frequency for different numbers of the used ferrite plates

As can be seen, the dependence of the impedance modulus on frequency is a constant function for frequencies $f < 200$ Hz. In this range, the value of the impedance modulus is determined by the winding resistance. In turn, the inductive character of the considered dependence is visible in a wide frequency range above 1 kHz. The use of ferrite plates causes an increase in the impedance modulus for $f > 1$ kHz resulting from an increase in the winding inductance. For different numbers of ferrite plats practically the same characteristics we obtained. This means that the use of additional ferrite plates changes neither the module characteristics nor the impedance phase. For a winding operating with a ferrite plate, there is a maximum in the frequency impedance characteristic of the module, and in the phase characteristic it is accompanied by a step change in the phase from 90° to –90°. This means the occurrence of resonance and a change in the winding impedance properties from inductive to capacitive. At resonance the value of overvoltage does not exceed 2 V.

Figure 5 illustrates the calculated and measured dependences of the module and the phase impedance of the receiver winding on frequency. As can be seen, the shape of these characteristics is similar to the characteristics presented in Fig. 4 for the transmitter winding. In both the cases, good agreement between the calculation and measurement results was obtained. This confirms the correctness of the developed model for individual windings. It is visible that for the number of ferrite plates higher than 1 practically no changes in obtained characteristics are visible. Therefore, in the next figures results obtained for transformers without any ferrite plate and with one plate only are presented.

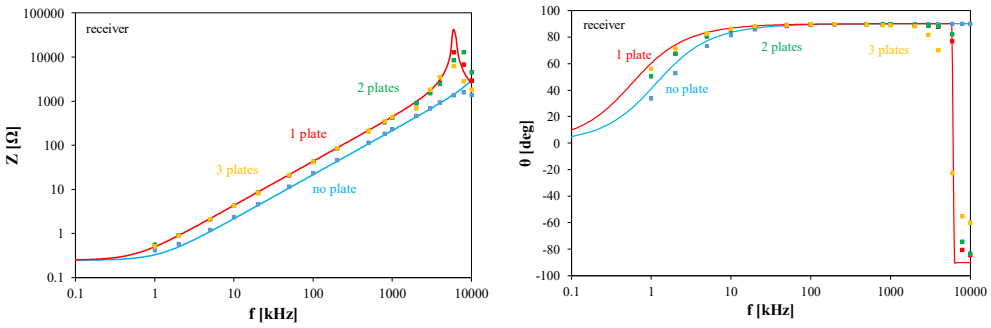

(a) (b)

Fig. 5. Measured and computed dependence of the module (a) and phase (b) of the impedance of the receiver winding on frequency for different numbers of the used ferrite plates

Figure 6 presents the dependence of the module and phase of the input impedance of the tested transformer on frequency when the receiving winding is loaded with a resistor of resistance 47 Ω. The investigations were performed with the coils adjacent to each other. The operation without ferrite plates and with such plates was considered.

As can be seen, there is both a minimum and a maximum in the dependence of the impedance modulus on frequency, indicating the occurrence of series and parallel resonance. For a transformer with ferrite plates, the maximum frequency occurs at a lower frequency than for a transformer without these plates. For both the constructions of the considered transformer, good agreement was obtained between the calculation and measurement results.

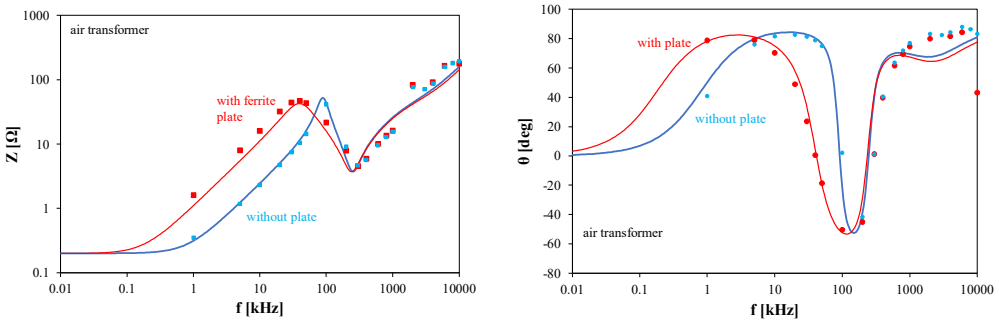

(a) (b)

Fig. 6. Measured and computed dependence of the module (a) and phase (b) of the input impedance of the tested air transformers on frequency

Analyzing the results presented in Figs. 4 and 5 it is easy to observe that parasitic capacitances of windings C_{P1} and C_{P2} visibly influence the presented characteristics for a frequency f higher than 1 MHz. In turn, an influence of capacitance C_m on the characteristics shown in Fig. 6 is visible for the values of a frequency higher than 10 kHz.

The following figures illustrate the results of large-signal investigations in the system shown in Fig. 3. These graphs illustrate the influence of frequency, load resistance, the distance between the windings and the presence of ferrite plates on the input voltage V_T and output voltage V_R of the investigated transformer. In the mentioned figures, solid lines and filled squares refer to V_T voltage, and dashed lines and unfilled squares refer to V_R voltage. All the presented results were obtained with a peak-to-peak supply voltage (at the power amplifier output) of 19 V.

Figure 7 illustrates the influence of frequency on voltages V_T and V_R at selected values of load resistance R_L. The characteristics presented in Fig. 7(a) refer to the transformer without ferrite plates, and in Fig. 7(b) – with ferrite plates.

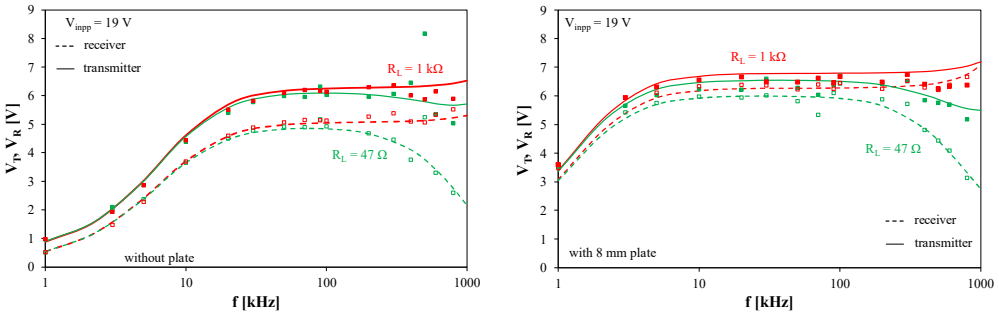

(a) (b)

Fig. 7. Measured and computed dependence of the input and output voltage on frequency at selected values of load resistance for the tested air transformers operating without any plate (a) and with the ferrite plate (b)

In Fig. 7(a) it can be seen that in the frequency range $f < 20$ kHz, the value of R_L resistance has practically no influence on the values of both the considered voltages. Clear differences in the shape of $V_T(f)$ and $V_R(f)$ waveforms obtained for both R_L resistance values are visible for

frequencies $f > 100$ kHz. The V_R voltage values obtained for $R_L = 47\ \Omega$ and $R_L = 1$ kΩ at frequency $f = 1$ MHz differ almost three times. $V_R(f)$ and $V_T(f)$ waveforms assume almost constant values in the frequency range from 20 to 100 kHz.

In turn, in Fig. 7(b) it can be seen that the use of ferrite plates allowed increasing the value of both the voltages by approximately 10% and extending the frequency range, in which the dependence of both the voltages on frequency is almost invisible. This range starts from 10 kHz. Comparing Figs. 7(a) and 7(b), it can be seen that the use of ferrite plates allowed for a significant (even fourfold) increase in the value of both the voltages in the low frequency range. This is due to a significant increase in the winding inductance when ferrite plates are used. In the high-frequency range, parasitic capacitances have the dominant influence on the considered characteristics, the values of which only slightly depend on the presence of ferrite plates. Therefore, in this respect, the differences between the characteristics of a transformer with and without ferrite plates are small.

Figure 8 presents transfer voltage characteristics of the tested transformer operating without any plate (Fig. 8(a)) and with such plate (Fig. 8(b)).

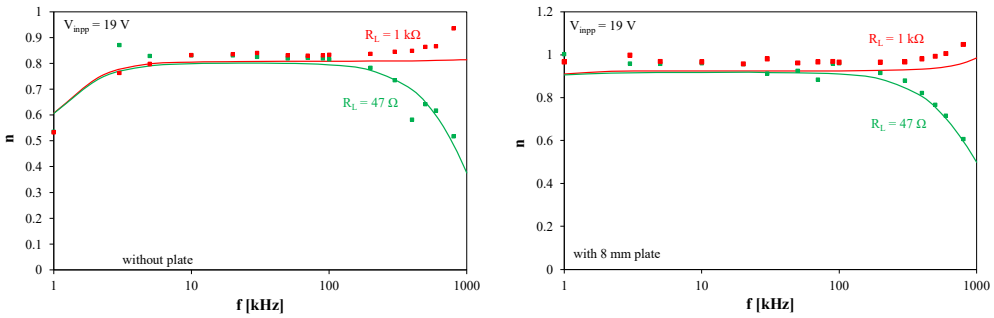

(a) (b)

Fig. 8. Measured and computed transfer voltage characteristics for the tested air transformers operating without any plate (a) and with the ferrite plate (b)

As it is visible, for the transformer operating without any plate the value of the voltage transfer is smaller than for this transformer with the ferrite plate. Such differences are mostly visible in the low-frequency range. An influence of the load resistance on the characteristics $n(f)$ is the biggest in the high-frequency range. The use of the ferrite plate makes it possible to obtain a high value of voltage transfer in a wide range of frequencies.

Figure 9 illustrates the influence of load resistance R_L on the voltage values V_R and V_T at selected frequency values. Figure 9(a) shows the transformer without ferrite plates, and Fig. 9(b) – with these plates.

It is worth noting that all the presented dependences $V_R(R_L)$ and $V_T(R_L)$ are monotonically increasing functions. A stronger influence of load resistance on V_R voltage is observed than on V_T voltage. This is related to the limited efficiency of energy transfer be-tween the transformer windings. In the considered frequency range, the presented wave-forms depend only slightly on the presence of ferrite plates. These plates only reduce the difference between the V_R and V_T voltage values. For a transformer without ferrite plates, this difference reaches 20%, and for a transformer with ferrite plates it is twice as small.

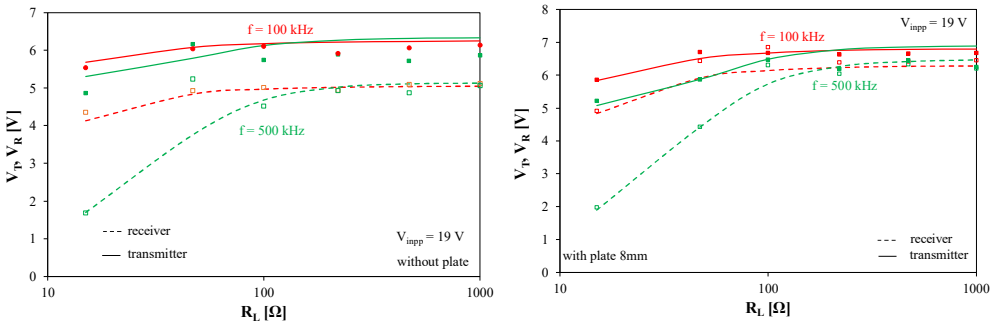

Fig. 9. Measured and computed dependence of the input and output voltage on load resistance at selected values of frequency for the tested air transformers operating without any plate (a) and with the ferrite plate (b)

Figure 10 illustrates the dependence of V_R and V_T voltages on the distance between the transformer coils with ferrite plates at selected values of load resistance and frequency.

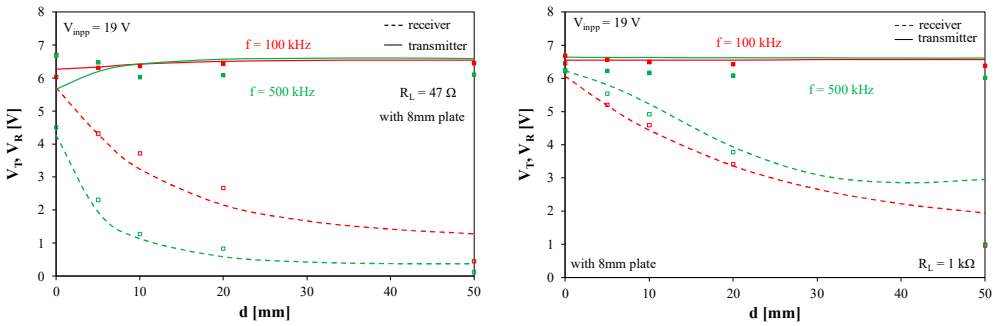

Fig. 10. Measured and computed dependence of the input and output voltage on the distance between the windings at selected values of frequency for the tested air transformers operating without any plate for load resistance equal to 47 Ω (a) and 1 kΩ (b)

As can be seen, the distance between the coils practically does not affect the voltage of the transmitting coil, but it strongly affects V_R voltage. Comparing the characteristics obtained with both the considered resistance values R_L, it can be seen that a decrease in the V_R voltage value with an increase in the distance between the coils is faster with a lower R_L resistance value. At a low value of load resistance, the energy transmission between the coils disappears when the distance between them is larger and the frequency is higher. With the same distance between the coils and the same frequency value, V_R voltages obtained at $R_L = 1$ kΩ are even 4 times higher than for $R_L = 47$ Ω.

Figure 11 illustrates the influence of the distance d between the coils on voltages occurring on both the windings of the investigated transformer operating without ferrite plates.

It can be seen that the value of voltage V_T practically does not depend on the distance d, while voltage V_R decreases exponentially with an increase in the value of d. The steepness of the V_R voltage drop is bigger with a higher resistance value R_L. At the lower of the considered resistance

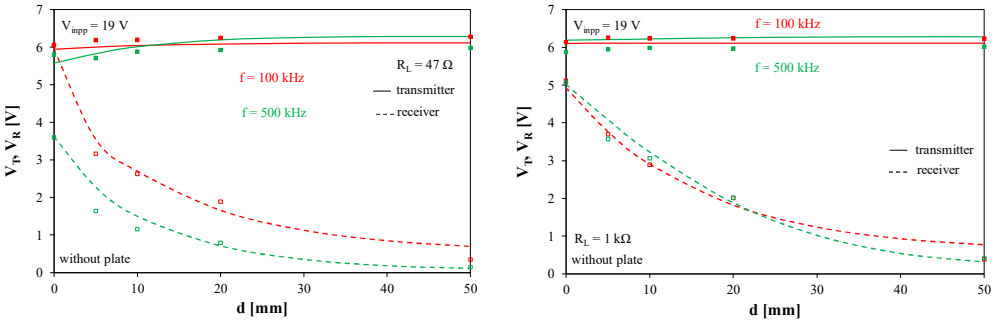

Fig. 11. Measured and computed dependence of the input and output voltage on the distance between the windings at selected values of frequency for the tested air transformers operating with the ferrite plate for load resistance equal to 47 Ω (a) and 1 kΩ (b)

values R_L, the influence of frequency on the course of the $V_R(d)$ relation-ship is visible. At this resistance value, an increase in frequency causes a drop in this voltage by up to 50%. Comparing the results presented in Figs. 9 and 10, it can be seen that with the same distance between the coils, a higher V_R voltage value is obtained when the transformer works with ferrite plates.

5. Conclusion

The paper presents the results of the experimental and simulation investigations illustrating the influence of selected factors on properties of air transformers with and without ferrite plates. A model of such a transformer dedicated to the SPICE program was formulated and its usefulness was demonstrated for determining frequency characteristics of the investigated transformers and for performing transient analyses of the systems with such transformers. It was shown that the developed model ensures good agreement between the calculated and measured characteristics of the investigated transformers.

The results of the investigations show that the use of ferrite plates increases the inductance of individual windings and increases their parasitic capacitances. The frequency characteristics of a transformer with or without ferrite plates have a similar shape. There are two extremes corresponding to parallel and series resonance. The differences between these characteristics are only quantitative. It is worth adding that the number of the used ferrite plates does not influence the obtained frequency characteristics of the windings and the transformer.

In the case of large-signal operation of the considered transformers when excited with a sinusoidal signal, it was observed that the voltage on the receiving winding decreases with an increase in frequency and the distance between the coils and with a decrease in load resistance. The use of ferrite plates increases the inductance of each winding and the coupling coefficient between them. The voltage values on the receiving coil in the low frequency range are much higher for a transformer with ferrite plates. The use of these plates also weakens the dependence of the coupling coefficient between the coils on the distance between them.

The presented results of the investigations and the proposed air transformer model may be useful for designers of wireless power transfer. This model will allow for a more detailed analysis of properties of the considered class of transformers.

Conventional applications of air transformers entail specific operating ranges, while in WPT systems there are current standardization. Within these operational ranges, compensation of coils utilizing capacitive networks occurs, necessitating a modification of the entire equivalent circuit. The properties of the considered class of networks depend on the transferred power and load resistance.

It is important to note that alterations in the coil and ferrite plate dimensions can impact the results due to resultant changes in mutual inductance. It is crucial to ensure that, if the core is not saturated, it operates within a linear region. These operational limits will be clarified in the future research using the finite element method (FEM) simulation.

When a ferrite plate is added to the air transformer, there is a concentration of the magnetic field within this medium. As a result, the mutual inductance and magnetic coupling factor visibly change. The specific description of these changes depends on several other factors, such as coils geometry and frequency. A model that accurately will represents this phenomenon have to be formulated and it should incorporate all significant variables as its parameters.

In our future works an influence of nonlinearities in magnetization characteristics of the used ferrite plate on the transformer conversion ratio will be investigated. Additionally, an influence of the shape and dimensions of ferrite plates on these characteristics will be analyzed.

References

[1] Krause C., *Power transformer insulation–history, technology and design*, IEEE Transactions on Dielectrics and Electrical Insulation, vol. 19, no. 6, pp. 1941–1947 (2012), DOI: 10.1109/TDEI.2012.6396951.

[2] Van den Bossche A., Valchev V., *Inductor and Transformers for Power Electronic*, CRC Press: Boca Raton, FL, USA (2005).

[3] Ericson R., Maksimovic D., *Fundamentals of Power Electronics*, Norwell; Kluwer Academic Publisher: Amsterdam, The Netherlands (2001).

[4] Valone T.F., *Geoengineering Tesla's Wireless Power Transmission*, ExtraOrdinary Science and Technology APR/MAY/JUN, pp. 31–42 (2017).

[5] Kurs A., Karalis A., Moffatt R., Joannopoulos J.D., Fisher P., Soljacic M., *Wireless power transfer via strongly coupled magnetic resonances*, Science, vol. 317, no. 5834, pp. 83–86 (2007), DOI: 10.1126/science.1143254.

[6] Coca E., *Wireless Power Transfer Fundamentals and Technologies*, InTechOpen (2016).

[7] Zhang Y., Yang J., Jiang D., Li D., Qu R., *Design, manufacture, and test of a rotary transformer for contactless power transfer system*, IEEE Transactions on Magnetics, vol. 58, no. 2, pp. 1–6 (2021), DOI: 10.1109/TMAG.2021.3094135.

[8] Kathirvelu K.P., Sandeep G.G.V., Swathi J., Amirtharajan R., Balasubramanian R., *Design of Transformer for wireless power transfer in electric vehicles*, Iranian Journal of Science and Technology, Transactions of Electrical Engineering, vol. 45, no. 4, pp. 1311–1324 (2021), DOI: 10.1007/s40998-021-00441-w.

[9] Detka K., Górecki K., *Wireless power transfer – a review*, Energies, vol. 15, no. 19, 7236 (2022), DOI: 10.3390/en15197236.

[10] Jayalath S., Khan A., *Design, Challenges, and Trends of Inductive Power Transfer Couplers for Electric Vehicles: A Review*, IEEE Journal of Emerging and Selected Topics in Power Electronics, vol. 9, no. 5, pp. 6196–6218 (2021), DOI: 10.1109/JESTPE.2020.3042625.

[11] Mou X., Sun H., *Wireless Power Transfer: Survey and Roadmap*, 2015 IEEE 81st Vehicular Technology Conference (VTC Spring), pp. 1–5 (2015), DOI: 10.1109/VTCSpring.2015.7146165.

[12] Rigot V., Phulpin T., Sadarnac D., Sakly J., *A new design of an air core transformer for Electric Vehicle On-Board Charger*, 2020, 22nd European Conference on Power Electronics and Applications (EPE'20 ECCE Europe), Lyon, France, pp. 1–9 (2020), DOI: 10.23919/EPE20ECCEEurope43536.2020.9215632.

[13] Bo L., Mao Z., Zhang K., Liu P., *Analysis and Optimal Design of a WPT Coupler for Underwater Vehicles Using Non-Dominated Sorting Genetic Algorithm*, Applied Sciences, vol. 12, no. 4, 2015 (2022), DOI: 10.3390/app12042015.

[14] Pugi L., Grasso F., Paolucci L., Luchetti L., Zini G., *Finite Element Analysis of Copper Wire for Wireless Power Transfer Applications*, 2022 IEEE 21st Mediterranean Electrotechnical Conference (MELECON), Palermo, Italy, pp. 801–806 (2022), DOI: 10.1109/MELECON53508.2022.9843033.

[15] Stankiewicz J., *Comparison of the efficiency of the WPT system using circular or square planar coils*, Przegląd Elektrotechniczny, vol. 97, no. 1, pp. 38–43 (2022), DOI: 10.15199/48.2021.10.08.

[16] Marcinek M., *Rezonansowy układ przekształtnikowy z aktywną stabilizacją punktu pracy w systemach bezstykowego przekazywania energii*, PhD thesis, Zachodniopomorski Uniwersytet Technologiczny w Szczecinie (in Polish), Szczecin (2015).

[17] Kevin L., *Comparative Study of Different Coil Geometries for Wireless Power Transfer*, Dissertation submitted for the Degree of Study (Hons), Universiti Teknologi PETRONAS (2016).

[18] Murakami R., Inamori M., Morimoto M., *Effects of Q factor on wireless power transmission by magnetic resonant coupling*, 2016 IEEE International Conference on Power and Renewable Energy (ICPRE), pp. 139–143 (2016), DOI: 10.1109/ICPRE.2016.7871189.

[19] International Electrotechnical Commission, IEC PAS 63095-2:2017(E), *The Qi wireless power transfer system – Power class 0 specification – Part 2: Reference Designs Version.1.1*, https://webstore.iec.ch/publication/28913, accessed 20 February 2024.

[20] *What is Qi2 wireless charging? And why you'll want it*, https://www.belkin.com/clp-what-is-qi2-wireless-charging-blog.html, accessed 20 February 2024.

[21] *How to Manage Loss Efficiently with Ferrite Tiles in Wireless Power Transfer*, https://www.kemet.com/en/us/technical-resources/how-to-manage-loss-efficiently-with-ferrite-tiles-in-wireless-power-transfer.html, accessed 21 February2024.

[22] *Ferrite Material, WPT Ferrite Tiles*, FPL Series, https://content.kemet.com/datasheets/KEM_FM0001_FPL (2023).

[23] *Ferrite plate*, https://www.mouser.pl/new/kemet-electronics/kemet-fpl-wpt-ferrite-tiles, accessed 28 January 2024.

[24] *Ferrite plate*, https://www.digikey.pl/pl/product-highlight/k/kemet/fpl-series-wpt-ferrite-tiles, accessed 28 January 2024.

[25] Wen H., Zhang C., *Investigation on transmission efficiency for magnetic materials in a wireless power transfer system*, 2015 IEEE 11th International Conference on Power Electronics and Drive Systems, pp. 249–253 (2015), DOI: 10.1109/PEDS.2015.7203423.

[26] Strauch L., Pavlin M., Bregar V.B., *Optimization, design, and modeling of ferrite core geometry for inductive wireless power transfer*, International Journal of Applied Electromagnetics and Mechanics, vol. 49, no. 1, pp. 145–155 (2015), DOI: 10.3233/JAE-150029.

[27] Agnaebrahimi M.R., Menzies R.W., *Air-core Transformer: A theoretical Analysis and Digital Simulations*, International Conference on Power Systems Transients IPST'97, Seattle, pp. 117–122 (1997).

[28] Liao Z.-J., Wu F., Jiang Ch.-H., Chen Z.-R., Xia Ch.-Y., *Analysis and Design of Ideal Transformer-Like Magnetic Coupling Wireless Power Transfer Systems*, IEEE Transactions on Power Electronics, vol. 37, no. 12, pp. 15728–15739 (2022), DOI: 10.1109/TPEL.2022.3191941.

[29] Fernández C., Prieto R., García O., Cobos J.A., *Coreless Magnetic Transformer Design Procedure*, 2005 IEEE 36th Power Electronics Specialists Conference, pp. 1548–1554 (2005), DOI: 10.1109/PESC.2005.1581836.

[30] ElGhanam E.A., Hassan M.S., Osman A., *Design and Finite Element Modeling of the Inductive Link in Wireless Electric Vehicle Charging Systems*, 2020 IEEE Transportation Electrification Conference & Expo (ITEC), Chicago, IL, USA, pp. 389–394 (2020), DOI: 10.1109/ITEC48692.2020.9161454.

[31] Shaarbafi K., *Transformer Modelling Guide*, Teshmont Consultants LP, https://www.aeso.ca/assets/linkfiles/4040.002-Rev02-Transformer-Modelling-Guide, accessed 2014.

[32] Özüpak Y., *Analysis of the Model Designed for Magnetic Resonance Based Wireless Power Transfer Using FEM*, Journal of Engineering Research, vol. 11, no. 3 (2023), DOI: 10.36909/jer.17631.

[33] Galarza R.J., Chow J.H., Degeneff R.C., *Transformer model reduction using time and frequency domain sensitivity techniques*, IEEE Transactions on Power Delivery, vol. 10, no. 2, pp. 1052–1059 (1995), DOI: 10.1109/61.400823.

[34] De Azambuja R., Brusamarello V.J., Haffner S., Porto R.W., *Analysis and optimization of an inductive power transfer with a randomized method*, IEEE Transactions on Instrumentation and Measurement, vol. 63, no. 5, pp. 1145–1152 (2014), DOI: 10.1109/TIM.2013.2296397.

[35] Guillod T., Czyz P., Kolar J.W., *Geometrical optimization of medium-frequency air-core transformers for DCX applications*, IEEE Journal of Emerging and Selected Topics in Power Electronics, vol. 10, no. 4, pp. 4319–4335 (2022), DOI: 10.1109/JESTPE.2021.3140197.

[36] Waters B.H., Sample A.P., Bonde P., Smith J.R., *Powering a ventricular assist device (VAD) with the free-range resonant electrical energy delivery (FREE-D) system*, Proceedings of the IEEE, vol. 100, no. 1, pp. 138–149 (2011), DOI: 10.1109/JPROC.2011.2165309.

[37] Detka K., Górecki K., Ptak P., *Model of an Air Transformer for Analyses of Wireless Power Transfer Systems*, Energies, vol. 16, no. 3, 1391 (2023), DOI: 10.3390/en16031391.

[38] Górecki K., Detka K., Górski K., *Compact thermal model of the pulse transformer taking into account nonlinearity of heat transfer*, Energies, vol. 13, no. 11, 2766 (2020), DOI: 10.3390/en13112766.

[39] Kazimierczuk M., Ayachit A., *Transfer functions of a transformer at different values of coupling coefficient*, IET Circuits, Devices and Systems, vol. 10, no. 4, pp. 337–348 (2016), DOI: 10.1049/iet-cds.2015.0147.

[40] Liu J., Deng Q., Czarkowski D., Kazimierczuk M.K., Zhou H., Hu W., *Frequency optimization for inductive power transfer based on AC resistance evaluation in litz-wire coil*, IEEE Transactions on Power Electronics, vol. 34, no. 3, pp. 2355–2363 (2019), DOI: 10.1109/TPEL.2018.2839626.

[41] Wojda R.P., Kazimierczuk M.K., *Winding resistance of litz wire and multi-strand inductors*, Proc. IET, Power Electronics, vol. 5, no. 2, pp. 257–268 (2012), DOI: 10.1049/iet-pel.2010.0359.

[42] Nagashima T., Wei X., Bou E., Alarcón E., Kazimierczuk M.K., Sekiya H., *Analysis and design of loosely inductive coupled wireless power transfer with class E2 dc-dc converter*, IEEE Transactions on Circuits and Systems – I, Regular Papers, vol. 62, no. 11, pp. 2781–2791 (2015), DOI: 10.1109/TCSI.2015.2482338.

[43] Pasko S.W., Kazimierczuk M.K., Grzesik B., *Self-capacitance of coupled toroidal inductors for EMI filters*, IEEE Transactions on Electromagnetic Compatibility, vol. 57, no. 2, pp. 216–223 (2015), DOI: 10.1109/TEMC.2014.2378535.

[44] Wojda R.P., Kazimierczuk M., *Winding resistance and power loss of inductors with litz and solid-round wires*, IEEE Transactions on Industry Applications, vol. 54, no. 4, pp. 3548–3557 (2018), DOI: 10.1109/TIA.2018.2821647.

[45] Mohan S.S., del Mar Hershenson M., Boyd S.P., Lee T.H., *Simple accurate expressions for planar spiral inductances*, IEEE Journal of Solid-State Circuits, vol. 34, no. 10, pp. 1419–1424 (1999), DOI: 10.1109/4.792620.

[46] Bensetti M., Kadem K., Pei Y., Le Bihan Y., Labouré E., Pichon L., *Parametric Optimization of Ferrite Structure Used for Dynamic Wireless Power Transfer for 3 kW Electric Vehicle*, Energies, vol. 16, 5439 (2023), DOI: 10.3390/en16145439.

[47] Liu G., Zhang G., Liu G., Wang H., Jing L., *Experimental and numerical study of high frequency superconducting air-core transformer*, Superconductor Science and Technology, vol. 34, no. 8, 085011 (2021), DOI: 10.1088/1361-6668/ac086f.

[48] Kapetanović I., Sarajlić N., Tešanović M., Kasumović M., *Numerical Solution for the Distribution of the Electromagnetic and Thermal Fields of an Air-core Transformer*, Journal of Energy-Energija, vol. 57, no. 4, pp. 424–439 (2008), DOI: 10.37798/2008574331.

[49] Hitchcock R.N., Stanton S.J., Levy S., Dollinger R., *Computer modeling of medium coupled resonant air core transformers including resistive losses*, Army Electronics Technology and Devices lab Fort Monmouth NJ (1983).

[50] *Ferrite plate type BHIP*, https://www.digikey.pl/pl/products/detail/kemet/FPL100-100-6-BH1T/10321373, accessed 28 January 2024.